Artificial Intelligence for Engineering Design, Analysis and Manufacturing (1998), *12*, 231–242. Printed in the USA.

PRACTICUM PAPER

The application of fuzzy neural network techniques in constructing an adaptive car-following indicator

PAI-CHUAN LU

Department of Mechanical Engineering, National Lien Ho College of Technology and Commerce, 1 Lien Kung Rd., Miaoli 36012, Taiwan, R. O. C.

(Received July 30, 1997; Accepted February 5, 1998)

Abstract

This paper proposes a fuzzy neural network (FNN) based approach to construct an individual-oriented car-following system. The feature of this system is firstly to incorporate a personal risk-taking factor in addition to other mechanical factors as the input parameters. Through the learning capability of artificial network, the complex membership functions between the input factors and the output (i.e., the appropriate car-following headway) can be efficiently established, and then the fuzzy logic rules can be properly constructed. The performance of the FNN system is finally assessed against the field data. The results are inspiring that the system is proven capable of providing highly accurate predictions of the required car-following headways from person to person at various speeds. The success of this study provides some clues of utilizing FNN techniques in exploring some individual-oriented machines.

Keywords: Car-following Indicator; FNN Techniques; Headways; Individual-oriented Machines; Neural Networks

1. INTRODUCTION

It is a known fact that a minimum space is required between cruising vehicles to prevent collision. The space between vehicles, on the other hand, influences roadway capacity which in turn affects the level of service to the users. In the past, several theories concerning vehicle spacing have been suggested (Pipes, 1953; Dobbins et al., 1962; Sakai & Nagao, 1969; Manheim, 1979; Roberston, 1979; Hulbert, 1982; Ross, 1985; Shenk, 1986); however, none of them ever involved any parameter that may reflect human performance. This is an important aspect in the consideration of traffic safety and efficiency. Traffic control devices may be employed to protect drivers, train prospective drivers adequately, and improve the behavior of violators only after a thorough understanding of driver behavior has been obtained.

This paper will mainly focus on constructing a fuzzy neural network (FNN) adaptive car-following system to remind drivers to keep proper spacings (headways) during cruises. Supposing that the driver is solely responsible for the state of the cruising vehicle, the actions of the driver play a significant role in the effectiveness of any designed-in safety device. However, measurement of driver performance, with respect to road safety, is a matter of great difficulty. Most of the difficulties lie on the methodology used in evaluating drivers' performance, especially with respect to safety-related decision behavior (Dobbins et al., 1961). Nevertheless, the drivers' decision-making skills may be rationally treated as a significant factor governing the interaction between the vehicle and its environment. These interactions ultimately determine the safety of the driver's actions. A previous paper (Lu, 1994) has successfully demonstrated the feasibility of introducing a risk-taking factor into the Pipes' equation (Pipes, 1953) to reflect individuality of drivers' behaviors. Accordingly, this work will broaden the basis to include risk-taking factor into the measurable mechanical factors (i.e., the speed of car and the free travel of the brake pedal) as the input parameters, while the desired car-following headway serves as the output. Fuzzy-neuro algorithm is then used to construct an individually oriented car-following indicator. Through testing, the indicator developed in this work has accurately signified the required person-to-person car-following headways at various speeds.

Reprint requests to: Pai-Chuan Lu, Department of Mechanical Engineering, National Lien Ho College of Technology and Commerce, 1 Lien Kung Rd., Miaoli 36012, Taiwan, R. O. C.; E-mail: pcl@alumni.nctu.edu.tw

2. THE INPUT FOR THE FUZZY NEURAL NETWORK

The speed of the car, the free travel of the brake pedal, and the individual risk-taking factor for drivers are the inputs for the FNN system. The risk-taking factor represents personal driving behaviors, while the others are closely related to mechanical responses of vehicles. It is only common sense that the required car-following headway must increase in proportion to the speed of vehicle. On the other hand, the free travel of the brake pedal shall determine the reaction time needed to activate the brake mechanism.

It is essential to conceive an appropriate expression for the risk-taking factor in driving behaviors before introducing this factor as one of the inputs for the FNN system. The previous work (Lu, 1994) created the following risk-taking factor in an aim to reflect reality:

$$\mu = \frac{1}{1 + a(R_b - D_b)^b}, \tag{1}$$

where R_b is the distance between the car and the obstacle when the brake is just applied; a and b are adjustable parameters, which can be determined from the field data collected through the computer program designed; while D_b is the required horizontal braking distance which can be expressed as (Drew, 1968)

$$D_b = \frac{v_0^2}{2g(f + G)}, \tag{2}$$

where v_0 is the speed when the brake is just applied; f is the coefficient of friction between the pavement and tires; G is the percent grade divided by 100; and g is the acceleration due to gravity.

It is designed such that when R_b is equal to D_b, the risk-taking factor μ reaches its maximum value of 1. This means that the driver is only bold enough to apply the brake when the car is away from the obstacle at the required minimum braking distance. As such, the risk-taking factor is rated at the highest level. On the other hand, as R_b increases, the corresponding risk-taking factor decreases. This coincides with the actual situations. The values of a and b ($a = 0.0169$, $b = 0.4971$) were determined in the previous work (Lu, 1994) by a designed computer program to fit the field data. Hence, in this work, Eq. (1) will still be utilized to evaluate the individual risk-taking factor as one of the inputs for the FNN system.

3. EXPERIMENT

Fifty experienced drivers were recruited from the Taiwan Highway Bureau and through newspaper advertisements for the study. Applicants had to meet the following criteria: 1) a minimum of 10 yr driving experience; 2) no record of serious traffic violation and accident; and 3) free from any alcohol, drug, or substance dependency that could impair driving ability. The average yearly mileage driven by applicants was 242,100 km. Individuals were briefed as to the nature of the study. They were asked to read an information letter describing the study and its associated benefits and risks. Qualified applicants who agreed to participate also signed a waiver indemnifying us from any liability obligation. Participants were then shown the research vehicle, and instructed on its operation. Before each trial, participants were asked to adjust the driver's seat and viewing mirrors, as well as required to fasten the seat belt. The tests used five different manual-transmission vehicles (Toyota Corolla, Ford Telstar, Toyota Tercel, Nissan Cefiro, Honda City); the free travel of the brake pedal was changed and recorded before every test. All the participants were randomly assigned to the five different vehicles, and each participant was made to drive the same vehicle throughout the tests.

Prior to field tests, each participant underwent a test at the Southern Technology Training Center (STTC) of the Taiwan Highway Bureau to determine the risk-taking factor on a straight lane (100 m long). A steel plate (2.5×1.5 m^2) obstacle was placed at the end of the lane. Then, a laser distance detector was mounted on the front license plate bracket of each test car to measure the distance between the car and the steel plate when brake was applied. The laser distance detector, along with a separate speed recorder installed in the car, were to be triggered simultaneously by the brake peddle. Both the laser distance detector and the speed recorder were connected to a Pentium notebook computer placed inside the test car. Once the driver applies the brakes upon approaching the steel plate, he activates the laser distance detector and speed recorder, which in turn simultaneously records the distance between the front end of the test car and the steel plate (R_b), as well as its speed (V_0) (as shown in Figure 1). This information was stored in the computer to determine the individual risk-taking factor. The drivers had to stop the car before it collides with the steel plate. The friction coefficient was estimated at 0.02 for the asphalt concrete lane (Wong, 1993). During the test, every participant accelerated the dormant car at the beginning of the lane and then shifted gears alternately from the first gear to the third gear before brake was applied. After the test was completed, the associate risk-taking factor for each participant was computed using Eqs. (1) and (2), according to the collected R_b, V_0 data.

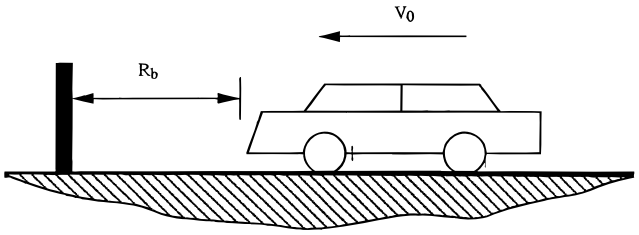

Fig. 1. The distance between the car and the obstacle when brake is applied.

https://doi.org/10.1017/S0890060498123028 Published online by Cambridge University Press

The field-test site was a newly paved, asphalt concrete highway in Tainan County, Taiwan. A 1990 four-door manual-transmission Toyota Corolla served as the leading car; it was driven by one of the experiment assistants. In each of the five different research cars, which were following, a switch was attached to the turn signal stalk. It was meant to simultaneously trigger the laser distance detector mounted on the front license plate bracket and the speed recorder. The notebook computer was connected to both the laser distance detector and the speed recorder for real-time data collection purposes.

In each trial, participants were separately instructed to drive along the predetermined route of the local highway. An experiment assistant sat on the passenger seat at all times, to give each participant route guidance. The following car was required to track the leading car all throughout the test route; the speed of the leading car was maintained between 30 km/h to 80 km/h. During all the cruises, when the participant in the following car felt capable of maintaining an appropriate headway (i.e., participants had no desire to accelerate or to decelerate), the participant had to press the switch on the turn signal stalk to record both the headway distance and the speed at that time. Tests were only performed when weather and road conditions permitted; data collection was done between the hours of 9:30 a.m. and 4:30 p.m. to avoid rush hours, when large fluctuations in traffic density are prevalent. At the end of each trial, participants returned to the STTC research facility. Only data for highway speed above 30 km/h were included in the analyses. Additional data, which included time spent driving to and from the STTC facility to the highway, were not included.

4. STRUCTURE OF THE FUZZY NEURAL NETWORK

The FNN adopted in this study is a feedforward multilayered network which integrates the basic elements and functions of a traditional fuzzy logic controller into a connective structure possessing distributed learning abilities. The fuzzy decision networks can be constructed from training patterns by machine learning techniques. The connective structure can be trained to develop fuzzy logic rules and to find optimal input/output membership functions. This connective model also provides human-understandable meaning to the normal feedforward multilayer neural network in which the internal units are always opaque to users. The advantage of bringing the learning abilities of neural networks to the fuzzy logic systems of this connective model is that it prevents the inference engine rule-matching time prevalent in traditional fuzzy logic systems; it also provides a promising approach.

Due to the nature of this work, the two-phase unsupervised/supervised learning algorithm (Lin & Lee, 1992) for the FNN was used. It combines unsupervised and supervised learning schemes to construct fuzzy neural networks automatically from training patterns. In phase I, a self-organized learning scheme is used to locate initial membership functions and to find the presence of rules. In phase II, a supervised learning scheme is used to optimally adjust the membership functions for desired outputs. By combining both unsupervised (self-organized) and supervised learning schemes, the learning speed converges much faster than in the original back-propagation learning algorithm since the self-organized learning process in phase I has done much of the learning work in advance.

4.1. Connective model

Figure 2 shows the connective FNN system of this work. The system has a total of five layers. y_1 is the output variable; it stands for the appropriate headway, while x_1, x_2, x_3 are the input variables representing the risk-taking factor, the speed of the car (km/h), and the free travel of the brake pedal (cm), respectively. Nodes in layer I are the input nodes representing input linguistic variables. Layer V is the output layer. Two linguistic nodes are provided for the single output variable. One is for training data (desired output) that is to be fed into this net, and the other is for decision signal (actual output) that is to be pumped out of this net. Nodes in layer II and layer IV are term nodes, which act as membership functions to represent the terms of the respective linguistic variables. Each node in layer III is a rule node, which represents one fuzzy rule. Therefore, all the layer III nodes form a fuzzy base. Links in layer III and layer IV serve as a connective inference engine that prevents the rule-matching process. Layer III links define the preconditions of the rule nodes, while layer IV links define the consequences of the rule nodes. For each rule node, there is, at most, one link (maybe none) from some term node of a linguistic node. The links in layer II and layer V are fully connected between the linguistic nodes and their corresponding term nodes. Figure 3 shows the basic functions of a node. Associated with the fan-in of a node is an integration function *f*, which serves to combine information from other nodes. This function provides the net input for this node.

$$\text{net} - \text{input} = f(u_1^k, u_2^k, \ldots, u_p^k; \omega_1^k, \ldots, \omega_p^k) \tag{3}$$

where the superscript indicates the layer number. A second node action is to output an activation value as a function of its net input

$$\text{output} = o_i^k = a(f) \tag{4}$$

where a$(\cdot)$ denotes the activation function. The functions f and a of the nodes in each of the five layers of this connective model are as follows:

Layer I:

$$f = u_i^1 \qquad \text{and} \qquad a = f \tag{5}$$

https://doi.org/10.1017/S0890060498123028 Published online by Cambridge University Press

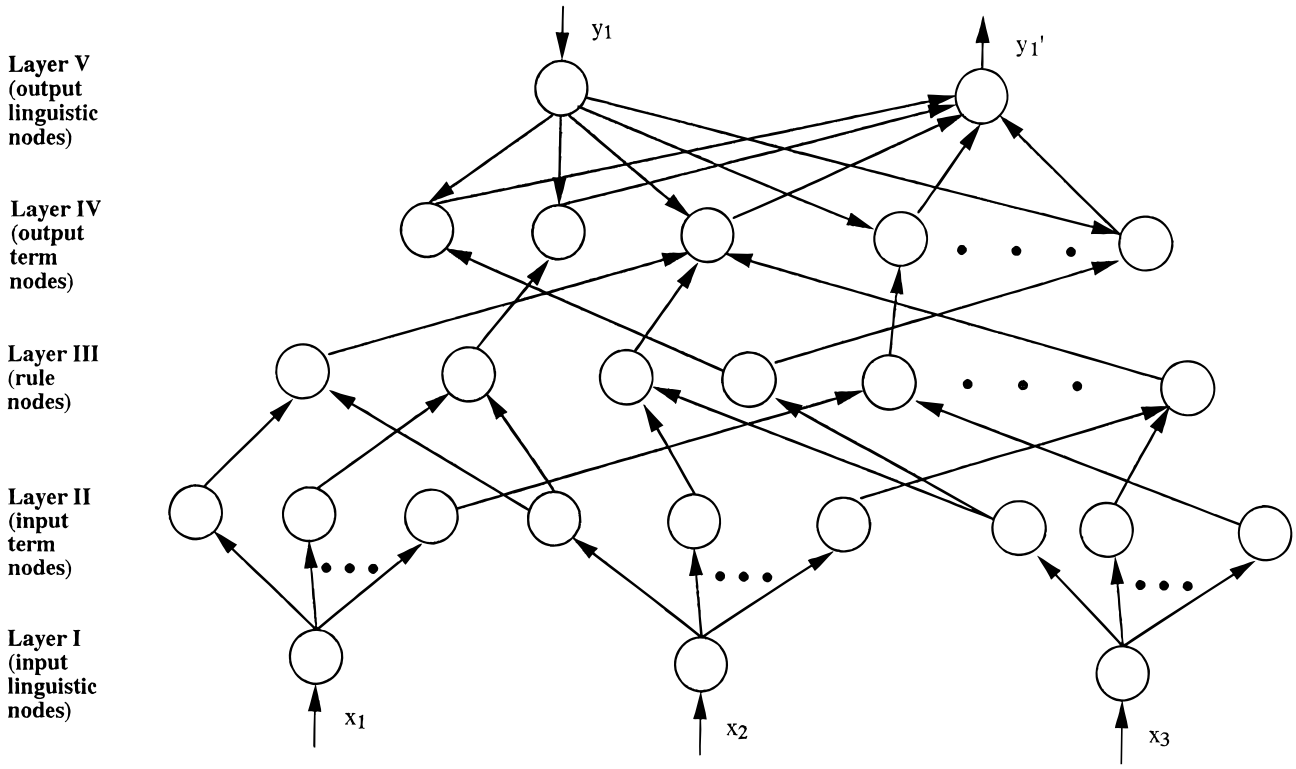

Fig. 2. The fuzzy neural network (FNN).

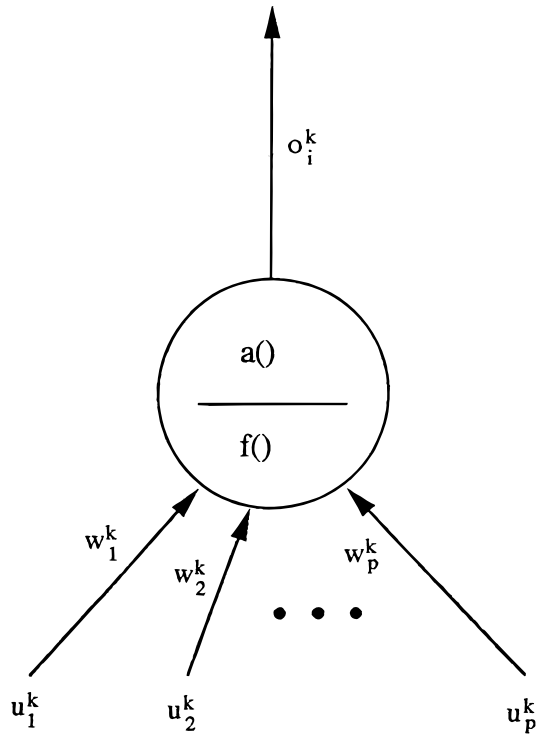

Fig. 3. Basic node structure in a neural network.

Layer II:

$$f = -\frac{(u_i^2 - m_{ij})^2}{\sigma_{ij}^2} \quad \text{and} \quad a = e^f \tag{6}$$

Layer III:

$$f = \min(u_1^3, u_2^3, \ldots, u_p^3) \quad \text{and} \quad a = f \tag{7}$$

Layer IV:

$$f = \sum_{i=1}^{p} u_i^4 \quad \text{and} \quad a = \min(1, f) \tag{8}$$

Layer V:

$$f = \Sigma \omega_{ij}^5 u_i^5 = \Sigma (m_{ij} \sigma_{ij}) u_i^5 \quad \text{and} \quad a = \frac{f}{\Sigma \sigma_{ij} u_i^5}. \tag{9}$$

Based on the above connective structure, this two-stage learning algorithm will determine the optimal centers (m_{ij}) and widths (σ_{ij}) of term nodes in layer II and layer IV. It will also learn fuzzy logic rules by deciding the existence and connection types of the links at layer III and layer IV.

https://doi.org/10.1017/S0890060498123028 Published online by Cambridge University Press

4.2. Self-organized learning phase

Given the training input data $x_i(t)$, $i = 1, \ldots, n$, the desired output value $y_i(t)$, $i = 1, \ldots, m$, the fuzzy partitions $|T(x)|$ and $|T(y)|$, and the desired shapes of membership functions, the task therefore is to locate the membership functions and to find the fuzzy logic rules. In this phase, the network works in a two-sided manner; that is, the nodes and links in layer IV are in the up–down transmission mode, so that the training input and output data are fed into this network from both sides.

The centers (means) and the widths (variances) of the membership functions are determined by self-organized learning techniques analogous to statistical clustering. Kohonen's feature-maps algorithm (Kohonen, 1988) is adopted to find the center m_i of the membership function.

$$\|x(t) - m_{\text{closest}}(t)\| = \min_{1 \le i \le k} \{\|x(t) - m_i(t)\|\} \tag{10}$$

$$m_{\text{closest}}(t+1) = m_{\text{closest}}(t) + \alpha(t)[x(t) - m_{\text{closest}}(t)] \tag{11}$$

$$m_i(t+1) = m_i(t), \qquad \text{for } m_i \neq m_{\text{closest}}, \tag{12}$$

where $\alpha(t)$ is a monotonically decreasing scalar learning rate, and $k = |T(x)|$. Once the centers of membership functions are found, their widths may then be determined through the N-nearest-neighbor heuristic, by minimizing the following objective function with respect to the widths σ_i.

$$E = \tfrac{1}{2}\sum_{i=1}^{N}\left[\sum_{j \in N_{\text{nearest}}}\left(\frac{m_i - m_j}{\sigma_i}\right)^2 - r\right]^2, \tag{13}$$

where r is an overlap parameter. Additionally, the widths can be simply determined by the first-nearest-neighbor heuristic at this stage as

$$\sigma_i = \frac{|m_i - m_{closest}|}{r}. \tag{14}$$

After the parameters of the membership functions are found, the signals from both external sides may reach the output points of term nodes in layer II and layer IV. Furthermore, the outputs of term nodes in layer II may be transmitted to rule nodes through the initial architecture of the layer III links; thereby providing the firing strength of each rule node. Based on the rule firing strengths $[o_i^3(t)]$ and the outputs of term nodes in layer IV $[o_j^4(t)]$, the correct rule node consequence links (layer IV links) for finding the existing fuzzy logic rule are decided by competitive learning algorithms. The following competitive learning law is used to update these weights for each training data set.

$$\dot{\omega}_{ij}(t) = o_j^4(-\omega_{ij} + o_i^3), \tag{15}$$

where ω_{ij} is the weight of the link between the ith rule node and the jth output term node, and o_j^4 serves as a win-loss index of the jth term node in layer IV.

The whole training data set was placed under competitive learning. The link weights in layer IV represent the strength of the corresponding rule consequence found. At most, one link with maximum weight is chosen from the links connecting a rule node to the term nodes of an output linguistic node, and the others are deleted. Hence, only one term in an output linguistic variable's term set can become a consequence of a fuzzy logic rule. If all the link weights between a rule node and the term nodes of an output linguistic node are very small, then all the corresponding links are deleted. This means that this rule node has little or no relation to this output linguistic variable. If all the links between a rule node and the layer IV nodes are deleted, then this rule node can be eliminated since it does not affect the outputs.

After the rule node consequences are determined, the rule combinations are performed to reduce the number of rules. The criteria for a set of rule nodes to be combined into a single rule node are 1) they have exactly the same consequences; 2) some preconditions are common to all the rule nodes in this set; and 3) the union of other preconditions of these rule nodes composes the whole term set of some input linguistic variables. If a set of nodes can meet these criteria, then only a new rule node possessing common preconditions may be used to replace this set of rule nodes. An example is illustrated in Figure 4.

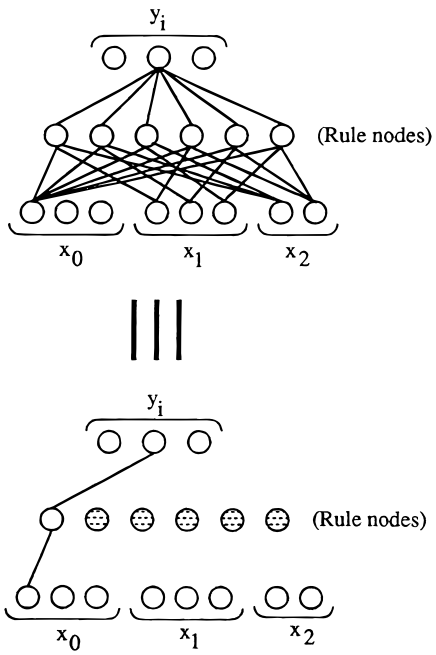

Fig. 4. Example of rule node combination.

https://doi.org/10.1017/S0890060498123028 Published online by Cambridge University Press

Furthermore, note that initially in layer III, as many as possible rule nodes were placed before training. However, the algorithm designed for rule node combination deleted the redundant rule nodes after training. On the other hand, with respect to layer IV, the number of nodes, which is related to the number of output pattern groups, is determined rationally by users' experiences; this is the same way used to determine the number of nodes in layer II.

4.3. Supervised learning phase

The whole network structure was established after the fuzzy logic rules were found. Network then proceeded to the second learning phase to adjust the parameters of the membership functions optimally. In the second learning phase, the network operation was in the feedforward manner; that is, the nodes and the links in layer IV were in the down–up transmission mode. The goal was to minimize the error function

$$E = \tfrac{1}{2}[y(t) - \hat{y}(t)]^2, \tag{16}$$

where $y(t)$ is the desired output, and $\hat{y}(t)$ is the current output. Assuming that ω is the adjustable parameter in a node (e.g., the center of a membership function), the learning rule used is

$$\Delta\omega \propto -\frac{\partial E}{\partial \omega} \tag{17}$$

$$\omega(t+1) = \omega(t) + \eta\left(-\frac{\partial E}{\partial \omega}\right), \tag{18}$$

where η is the learning rate, and

$$\begin{aligned}\frac{\partial E}{\partial \omega} &= \frac{\partial E}{\partial(\text{net} - \text{input})}\frac{\partial(\text{net} - \text{input})}{\partial \omega} \\ &= \frac{\partial E}{\partial f}\frac{\partial f}{\partial \omega} \\ &= \frac{\partial E}{\partial a}\frac{\partial a}{\partial f}\frac{\partial f}{\partial \omega}.\end{aligned} \tag{19}$$

Bell-shaped membership functions with centers m_i and widths σ_i are used as the adjustable parameters in all the computations. The derivatives of the error function E for each layer is illustrated as follows:

Layer V. From Eq. (19) and Eq. (9), the adaptive rule of the center m_i is

$$\begin{aligned}\frac{\partial E}{\partial m_i} &= \frac{\partial E}{\partial a}\frac{\partial a}{\partial f^5}\frac{\partial f^5}{\partial m_i} \\ &= -[y(t) - \hat{y}(t)]\frac{\sigma_i u_i}{\Sigma \sigma_i u_i}.\end{aligned} \tag{20}$$

The center parameter is updated by

$$m_i(t+1) = m_i(t) + \eta[y(t) - \hat{y}(t)]\frac{\sigma_i u_i}{\Sigma \sigma_i u_i}. \tag{21}$$

Similarly, the adaptive rule of the width σ_i is

$$\begin{aligned}\frac{\partial E}{\partial \sigma_i} &= \frac{\partial E}{\partial a}\frac{\partial a}{\partial f^5}\frac{\partial f^5}{\partial \sigma_i} \\ &= -[y(t) - \hat{y}(t)]\frac{m_i u_i(\Sigma \sigma_i u_i) - (\Sigma m_i \sigma_i)u_i}{(\Sigma \sigma_i u_i)^2}.\end{aligned} \tag{22}$$

The width parameter is updated by

$$\sigma_i(t+1) = \sigma_i(t) + \eta[y(t) - \hat{y}(t)]\frac{m_i u_i(\Sigma \sigma_i u_i) - (\Sigma m_i \sigma_i u_i)u_i}{(\Sigma \sigma_i u_i)^2}. \tag{23}$$

The error to be propagated to the preceding layer is

$$\delta^5 = -\frac{\partial E}{\partial f^5} = -\frac{\partial E}{\partial a}\frac{\partial a}{\partial f^5} = y(t) - \hat{y}(t). \tag{24}$$

Layer IV. In this layer, only the error signals (δ_i^4) need to be computed and propagated. The δ_i^4 is derived by

$$-\delta_i^4 = -\frac{\partial E}{\partial f_i} = -\frac{\partial E}{\partial a_i}\frac{\partial a_i}{\partial f_i} = \frac{\partial E}{\partial(\text{net} - \text{input})^5}\frac{\partial(\text{net} - \text{input})^5}{\partial a_i}, \tag{25}$$

where [from Eq. (9)]

$$\frac{\partial(\text{net} - \text{input})^5}{\partial a_i} = \frac{\partial f^5}{\partial u_i^5} = \frac{m_i \sigma_i(\Sigma \sigma_i u_i) - (\Sigma m_i \sigma_i u_i)\sigma_i}{(\Sigma \sigma_i u_i)^2} \tag{26}$$

and from Eq. (24)

$$\frac{\partial E}{\partial(\text{net} - \text{input})^5} = \frac{\partial E}{\partial f^5} = -\delta^5 = -[y(t) - \hat{y}(t)]. \tag{27}$$

Hence, the error signal is

$$\delta_i^4(t) = [y(t) - \hat{y}(t)]\frac{m_i \sigma_i(\Sigma \sigma_i u_i) - (\Sigma \sigma_i u_i)\sigma_i}{(\Sigma \sigma_i u_i)^2}. \tag{28}$$

Layer III. In this layer, only the error signals need to be calculated. According to Eq. (8), the error signal is

$$\begin{aligned}-\delta_i^3 &= \frac{\partial E}{\partial f_i} = \frac{\partial E}{\partial a_i}\frac{\partial a_i}{\partial f_i} \\ &= \frac{\partial E}{\partial(\text{net} - \text{input})^4}\frac{\partial(\text{net} - \text{input})^4}{\partial a_i} \\ &= -\delta_i^4\frac{\partial f^4}{\partial u_i^4} \\ &= -\delta_i^4.\end{aligned} \tag{29}$$

https://doi.org/10.1017/S0890060498123028 Published online by Cambridge University Press

Hence, the error signal is $\delta_i^3 = \delta_i^4$.

Layer II. From Eq. (19) and Eq. (6), the adaptive rule of m_{ij} can be derived from

$$\frac{\partial E}{\partial m_{ij}} = \frac{\partial E}{\partial a_i}\frac{\partial a_i}{\partial f_i}\frac{\partial f_i}{\partial m_{ij}} = \frac{\partial E}{\partial a_i} e^{f_i}\frac{2(u_i - m_{ij})}{\sigma_{ij}^2}, \tag{30}$$

where [from Eq. (29)]

$$\frac{\partial E}{\partial a_i} = \sum_k \frac{\partial E}{\partial (\text{net} - \text{input})^k}\frac{\partial (\text{net} - \text{input})^k}{\partial a_i} \tag{31}$$

$$\frac{\partial E}{\partial (\text{net} - \text{input})^k} = \frac{\partial E}{\partial f_k^3} = \delta_k^3 \tag{32}$$

and from Eq. (7),

$$\frac{\partial (\text{net} - \text{input})^k}{\partial a_i} = \frac{\partial f^3}{\partial u_i^3}. \tag{33}$$

Equation (33) is equal to 1 only if u_i^3 is identical to the minimum input of rule node k. Otherwise, Eq. (33) is equal to 0. Hence,

$$\frac{\partial E}{\partial a_i} = \sum_k q_k, \tag{34}$$

where the summation is performed over the rule node destinations of a_i, and q_k is equal to δ_k^3. a_i should be minimum in kth rule node's inputs; otherwise, q_k is equal to 0. Hence, the adaptive rule of m_{ij} is

$$m_{ij}(t+1) = m_{ij}(t) - \eta\frac{\partial E}{\partial a_i} e^{f_i}\frac{2(u_i - m_i)}{\sigma_{ij}^2}. \tag{35}$$

Likewise, the following is obtained from Eqs. (19), (6), and (31),

$$\frac{\partial E}{\partial \sigma_{ij}} = \frac{\partial E}{\partial a_i}\frac{\partial a_i}{\partial f_i}\frac{\partial f_i}{\partial \sigma_{ij}} = \frac{\partial E}{\partial a_i} e^{f_i}\frac{2(u_i - m_{ij})^2}{\sigma_{ij}^3}. \tag{36}$$

Hence, the adaptive rule of σ_{ij} becomes

$$\sigma_{ij}(t+1) = \sigma_{ij}(t) - \eta\frac{\partial E}{\partial a_i} e^{f_i}\frac{2(u_i - m_{ij})^2}{\sigma_{ij}^3}. \tag{37}$$

As in all other neural network training, the entire FNN's learning process is terminated once the learning error is less than the criteria designated value. Then, the learned fuzzy logic rules can be easily read from the final structure of the FNN. In particular, there is only one error criterion needed in the entire FNN learning process.

In establishing the data base for the fuzzy neural network, 3526 field data were collected, but only half of them would be used for training; the others were employed for testing after the network has been well trained.

5. RESULTS AND DISCUSSION

Once FNN has been trained, it was tested by the data from the data base that were not included in the training process. Figure 5 shows the learned membership functions of x_1, x_2, x_3, and y after phase I and phase II of the learning process. Based on these membership functions, it was able to construct further fuzzy logic rules. Figure 6 shows the curve of the mean error with respect to the number of epochs. The learning rate was set at 0.1 and the error tolerance is 0.01. The convergence mean error decreases dramatically at the beginning; this means that the phase I of the learning pro-

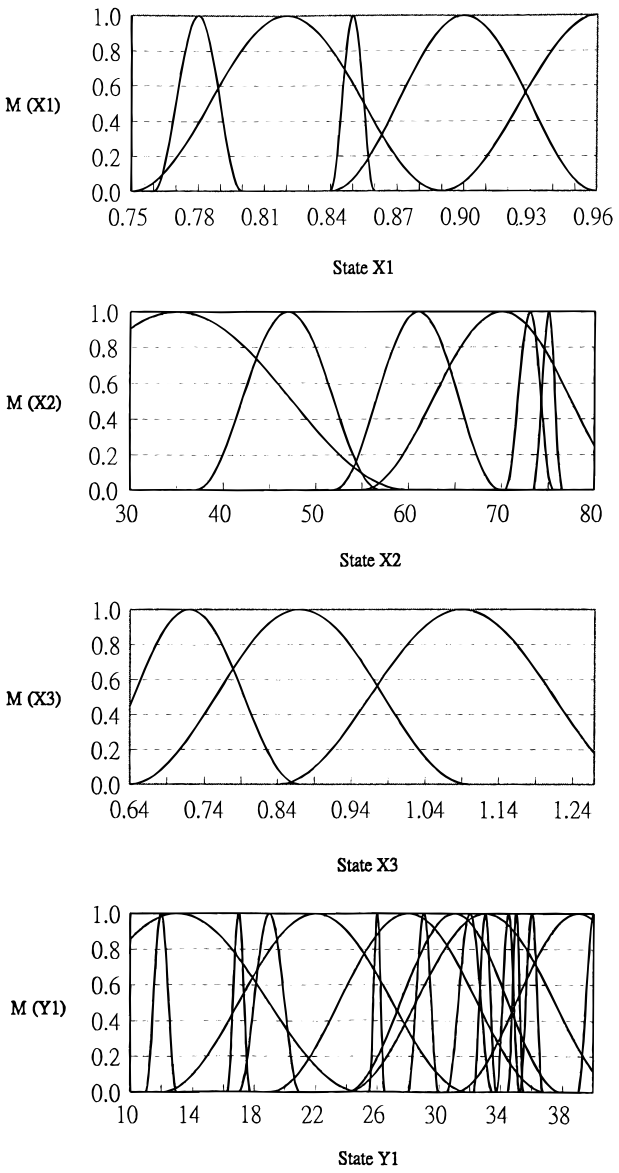

Fig. 5. Learned membership functions.

https://doi.org/10.1017/S0890060498123028 Published online by Cambridge University Press

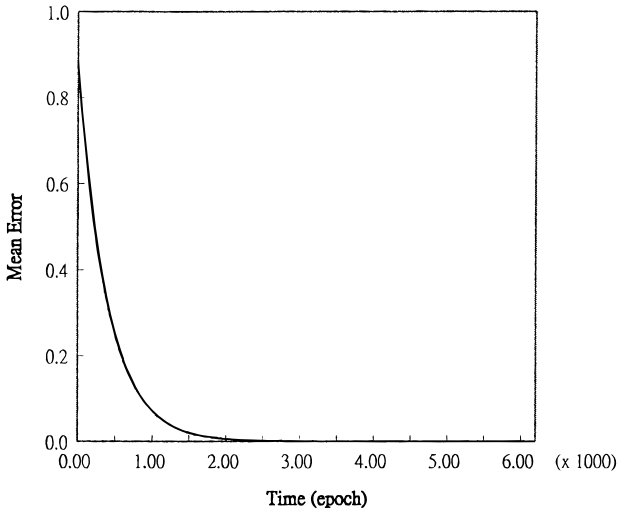

Fig. 6. Learning curve: mean error versus time (epoch).

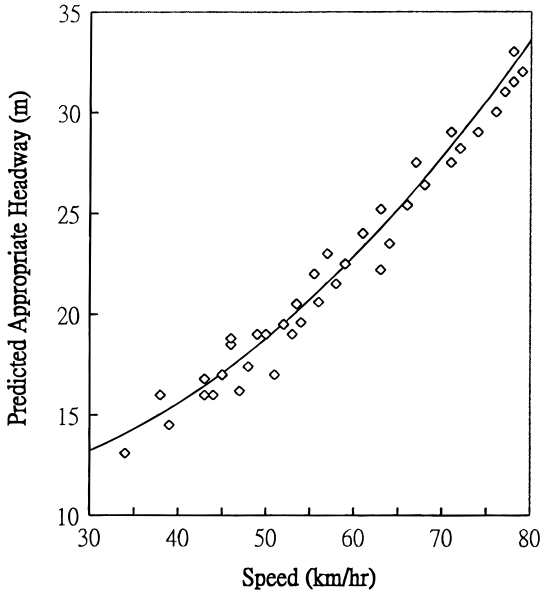

Fig. 8. The FNN headway predictions for the participant with a 0.87 risk-taking factor (μ).

cess shared much of the learning work. Finally, it used the trained net to perform predictions in conditions where one input variable is changed within a given range, while the other variables remained constant.

Figures 7–9 show the appropriate headways predicted by the FNN system for the three participants, when individual risk-taking factors were at 0.83, 0.87, and 0.92, respectively. The three participants drove the same test car in the experiment; free travel of the brake pedal was at 1.2 cm. The speed variations from Figures 6–8 ranged from 30 km/h to 80 km/h in conformity with the range of data collection. In these figures, FNN predicted that the appropriate headway shall increase if speed increases. The predicted values well agree with the data measured as shown. The arithmetic mean errors between the measured and the predicted headways are 4.5%, 3.7%, and 2.9%, respectively. For the participant showing a risk-taking factor of 0.92, the effect of speed on the appropriate headway was modest at low speeds; however, the appropriate headway increased sharply as speed increased at high speed level. This phenomenon could probably explain the high decision-making variability noted in the participants belong-

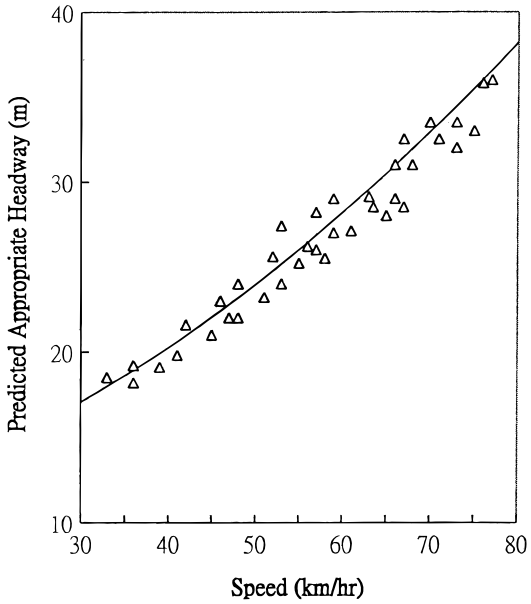

Fig. 7. The FNN headway predictions for the participant with a 0.83 risk-taking factor (μ).

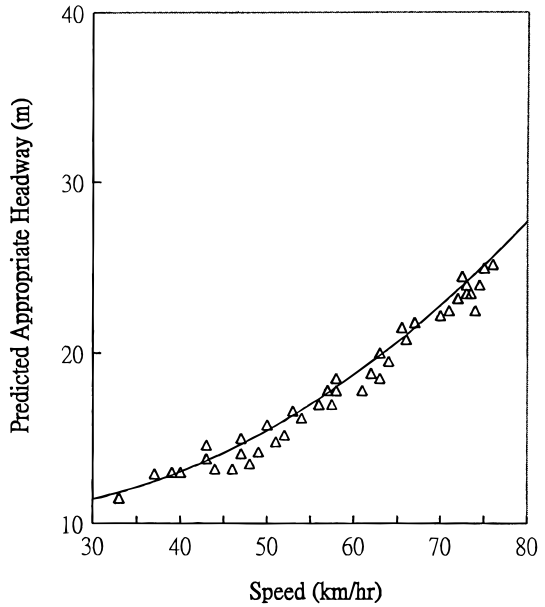

Fig. 9. The FNN headway predictions for the participant with a 0.92 risk-taking factor (μ).

https://doi.org/10.1017/S0890060498123028 Published online by Cambridge University Press

ing to the high risk-taking group. The comparison between the appropriate headways for the said three participants, and that of a participant having a 0.94 risk-taking factor, is shown in Figure 10. It revealed that participants with higher risk-taking factors needed smaller distance headways, and this was noted throughout the same range of data collection. However, it was also noted that, for the participants with higher risk-taking factors, the variation in the appropriate headway changing rate, with respect to speed, was larger when speed ranged from 30 km/h to 80 km/h. Table 1 shows the ratio of FNN prediction errors against measured data made on each participant's performance at different speed levels, ranging from 30 km/h to 80 km/h. The maximum prediction error rate noted in all the participants is less than 9%; while average error rate is less than 4.5%. Furthermore, test data were not included in the training stage; hence, based on the level of prediction errors, the performance of the system is found to be outstanding.

Table 1. *The FNN prediction errors against mesured data of each participant*

Participant number	Max. error (%)	Min. error (%)	Average error (%)
1	7.7	2.3	3.5
2	5.4	1.2	2.4
3	8.6	3.5	4.5
4	8.9	2.6	4.2
5	8.0	2.5	3.7
6	4.8	1.2	3.1
7	3.9	2.2	3.6
8	4.5	2.1	2.9
9	4.7	3.1	3.4
10	4.9	2.8	3.7
11	4.8	2.2	2.9
12	4.9	2.1	2.5
13	4.7	1.8	2.8
14	5.6	3.6	4.4
15	6.8	3.7	4.5
16	5.6	2.0	3.4
17	5.9	2.8	4.3
18	3.5	2.3	2.9
19	6.5	2.5	3.8
20	8.6	3.5	4.3
21	5.1	1.3	2.7
22	5.4	1.9	2.8
23	7.6	2.6	3.7
24	8.9	3.8	4.5
25	7.8	2.3	3.8
26	8.9	2.3	4.2
27	7.5	2.6	3.7
28	8.7	3.2	4.2
29	4.8	1.1	2.1
30	7.9	2.1	3.4
31	8.1	1.5	3.6
32	5.1	1.3	2.4
33	6.2	1.4	2.5
34	3.9	0.7	1.6
35	7.2	2.1	3.6
36	8.9	3.2	3.8
37	8.5	2.5	4.0
38	4.7	1.2	1.9
39	5.7	1.2	2.4
40	5.7	1.1	2.5
41	7.2	2.2	3.5
42	7.5	2.1	3.4
43	6.8	1.5	2.9
44	7.3	2.7	3.5
45	7.9	2.7	3.7
46	8.7	3.4	4.2
47	9.0	3.5	4.4
48	8.8	2.9	4.5
49	6.1	1.5	2.9
50	6.7	2.3	3.2

The effect of the risk-taking factors on the headways at various speeds is illustrated in Figure 11. As expected, the predicted appropriate headways decrease as the risk-taking factors increase. It has to be noted that from the design of this work, each person is supposed to have an individual risk-taking factor. The curves in Figure 11 show the trends of the predicted appropriate headways for various persons at different speed levels. Figure 11 also shows that the predicted appropriate headways increased as the controlled speed increased.

The trend prediction capability of this FNN system for brake pedal free travel and the appropriate headway is limited by the amount of data collected. In this research, only five different test cars, as mentioned in the above, were chosen. Before each test was started, the brake pedal free travel of each car was given a mechanism screw adjustment. There was a total of 50 brake pedal free travel data acquired from the tests. The FNN system cannot adequately make quality predictions concerning the effect of the brake pedal free travel on the appropriate headway from such minimal data.

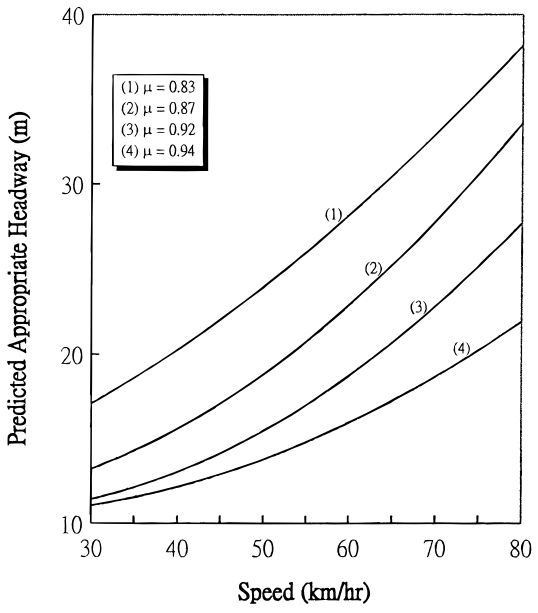

Fig. 10. The effect of speed levels on the headways at various risk-taking factors.

https://doi.org/10.1017/S0890060498123028 Published online by Cambridge University Press

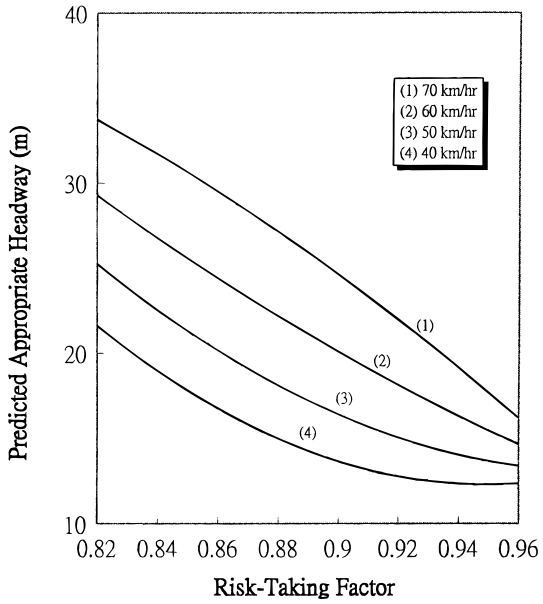

Fig. 11. The effect of the risk-taking factors on the headways at various speed levels.

Thus, the expansion of the data base shall become one of main tasks that future research needs to accomplish.

The prototype of the FNN car-following indicator is illustrated in Figure 12. The three parameters x_1, x_2, and x_3, as mentioned earlier, are fed into the fuzzifier by means of the risk-taking factor evaluator, the speed sensor, and the brake pedal free travel sensor. Through fuzzy inference, the predicted appropriate headway distances (y) at various speed levels are obtained. The predicted headways will then be compared with the actual headways (y') measured at mean time by the laser distance detector mounted on the front license plate bracket of the car. If the measured value (y') is less than the predicted appropriate value (y), then the system will activate a signal (z) to the warning alarm to remind the driver to slow down.

The significant advantage of FNN over the original backpropagation learning algorithm is that the FNN's learning speed converges much faster. The learning time includes the time spent on unsupervised and supervised learning. In fact, the portion of time spent on unsupervised learning is very little compared to the time spent on supervised learning. This study also attempted using the original backpropagation to learn the same data. It took around 1 wk to converge, whereas with the FNN, it took only $2\frac{1}{2}$ h to converge. Both procedures were executed using the same personal computer. The learning time saved by FNN is dramatic and could be over two orders. The other significant advantage of FNN is its readable structure. FNN's connective model provides human-understandable meaning to the normal feedforward multilayer neural network in which the internal units are always opaque to users. Of course, these FNN advantages means increased number of layers, which in turn, results in the complexity of the network. However, when viewed from the learning time saved and the readable structure point of view, it is worth the effort.

Furthermore, it was noticed that all the existing car-following models are incapable of modelling the risk-taking behavior of drivers. The previous work (Lu, 1994) modified the conventional Pipes' equation into a speed nonlinear form, which involved the risk-taking factor defined by Eq. (1). The input variables used were the risk-taking factor and the speed. The desired headways predicted by the modified model are close to the results shown in Figure 10. However, the key issue in this work is that none of the car-following models will be framed as prerequisite; only the designed risk-taking factor is utilized to describe the character of driver's behavior. After taking the brake pedal free travel and vehicle speed together with the risk-taking factor, the FNN system automatically starts with the prediction process.

In the future, two pressing issues have to be investigated to improve the system; one is the involvement of more vehicle condition parameters in addition to the brake pedal free travel as input parameters. The hydraulic pressure in the brake line, brake torque at the wheel, lining wear, and so on, may also be used as parameters to achieve results possessing higher levels of confidence. This means that more sensors have to be designed and installed in the proper areas of the vehicle to measure the additional parameters. The other issue is to conceive an alternative approach to conveniently determine the person-oriented risk-taking factor, to replace the current approach which needs to perform the

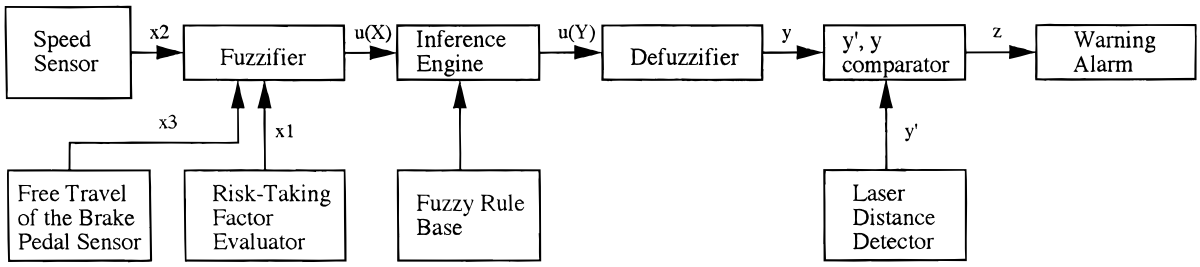

Fig. 12. The structure of the FNN car-following Indicator.

https://doi.org/10.1017/S0890060498123028 Published online by Cambridge University Press

braking test on a straight lane. Furthermore, the impact of the closing rate which the vehicle is achieving on the safe headway should also be explored in future studies.

As shown in this paper, the FNN system can be of great use in predicting the individual appropriate headway of a cruising car, and in giving the driver warning signals. A properly designed and trained FNN system is an efficient tool for establishing appropriate headway trends. Three features are required to achieve this goal: 1) a good knowledge of the problem, including the confirmation of the input parameters; 2) an extensive and accurate data base; and 3) an awareness of the limitations and possibilities offered by FNN. With regards to the latter, it is necessary to be aware of the limitations of the different topologies or designs, learning rules, and training time, when assessing the FNN predictive capabilities.

ACKNOWLEDGMENTS

The research for this article was carried out at The Laboratory of the Southern Technology Training Center of Taiwan Highway Bureau in Miaoli, Taiwan, R.O.C. The author gratefully acknowledges the assistance of the South Technicians Training Center, Taiwan Highway Bureau, and the support of the National Science Council of Taiwan under the Grant No. NSC 88-2212-E-239-001. Special thanks are due to Professor C. T. Lin of the National Chiao-Tung University of Taiwan for his invaluable comments on this work. The author would also like to thank J. K. Lin and J. C. Chen, who performed the experiments and data collection for this project.

REFERENCES

Dobbins, D.A., Skordahi D.M., & Anderson, A.A. (1961). *AASHO Road Test 119*, 131–145.

Dobbins, D.A., Skordahi D.M., & Anderson, A.A. (1962). *Human Factors Research Report—AASHO Road Test: II*. Highway Res. Board Bull., Washington, DC, pp. 330–341.

Drew, D.R. (1968). *Traffic Flow Theory and Control*, pp. 45–61. McGraw-Hill Corp., New York.

Hulbert, J. (1982). Human factors in transportation. *Transportation and Traffic Engineering Handbook*. Institute of Transportation Engineer, Washington, DC, pp. 121–134.

Kohonen, T. (1988). Self-organization and associative memory, pp. 132–143. Springer-Verlag, Berlin.

Lin, C.T. & Lee, C.S.G. (1992). Real-time supervised structure/parameter learning for fuzzy neural network. Proc. of IEEE Int'l Conf. on Fuzzy Systems. pp. 1283–1290. San Diego, CA.

Lu, P.C. (1994). *Successfully introducing the risk-taking factor into the conventional car-following model*. Technical Report (STTC-CS-85TP-4916). The South Technicians Training Center of the Taiwan Highway Bureau, Taiwan.

Manheim, M.L. (1979). *Fundamentals of Transportation System Analysis*, pp. 113–115. The M.I.T. Press, Cambridge, Massachusetts.

Pipes, L.A. (1953). An operational analysis of traffic dynamics. *Journal of Applied Physics 24 (3)*, 227–281.

Roberston, D.I. (1979). Traffic models and optimum strategies of control—a review. *Proceedings on Traffic Control Systems, 1*, 276–289.

Ross, R. (1985). Development, philosophies, and implications. *Transportation Research Record 971*. Transportation Research Board, Washington, DC, pp. 31–46.

Sakai, T., & Nagao, M. (1969). Simulation of traffic flows in a network. *Commun. ACM 12(6)*, 311–318.

Shenk, E. (1986). *Highway Capacity Software, User's Manual*, pp. 57–60. Polytechnic University, Brooklyn, New York.

Wong, J.Y. (1993). *Theory of Ground Vehicles*. 2nd ed., pp. 171–173. John Wiley & Sons, New York.

Pai-Chuan Lu is an Associate Professor in the Department of Mechanical Engineering at the National Lien Ho College of Technology and Commerce. His research and published papers to date have been in the field of fracture mechanics, stress corrosion, neural network, optimum design, and vehicle engineering. Dr. Lu has currently conducted several projects, including the one from the National Science Council of Taiwan. He received a Ph. D. degree in Engineering Science and Mechanics in 1994 from the Penn State University in the United States. Dr. Lu is also a member of the Phi Kappa Phi Honor Society. He received the Award of Academic Excellence from the Penn State University in 1994, and the Outstanding Research Award from the National Science Council of Taiwan in 1997.